

Impact of Greening Area Ratio on Urban Climate in Hot-summer and Cold-winter City

Qinli Deng¹, Zeng Zhou², Chuancheng Li³, Akashi Mochida⁴



¹ *Tohoku University, Aoba 6-6-11-1206, Sendai, Japan, deng@sabine.pln.archi.tohoku.ac.jp*

² *Wuhan University, Wuhan, Hubei province, China, haomaoz@hotmail.com*

³ *Wuhan University of Technology, Wuhan, Hubei province, China, chuanchengli@163.com*

⁴ *Tohoku University, Aoba 6-6-11-1202, Sendai, Japan, mochida@sabine.pln.archi.tohoku.ac.jp*

1. Introduction

The urbanization of land is rapidly increasing on a global basis, and the percentage of humans living in urban areas continues to grow worldwide. A study by the United Nations found that by 2050, 69.6% of the world's population will live in cities, as compared to 48.6% in 2005.[1] In recent years, China has been subject to a significant degree of urbanization, and the heat island effect has become increasingly serious in many large Chinese cities.

Many studies have focused on the influence of urbanization on the urban climate/meteorological environment and synoptic/climate processes, urban heat islands, contributions of urban environments to global warming, and reduced air moisture and evaporation in cities.

Jin et al.[2] examined three cities to illustrate the variations of these variables with land cover under different climate conditions, and found that urban areas were characterized by albedos much lower than those of croplands and deciduous forests in summer but similar to those of forests in winter. Li et al.[3] examined the climate effect of urbanization in Yangtze River Delta of China, and found that the urbanization not only can raise skin temperature and reduce diurnal temperature range and near surface wind speed in urbanized areas, but can increase diurnal temperature range in some suburban areas. Zhang et al.[4] developed a new model (Regional Atmospheric Modeling System- Urban Canopy) to analyze the heat island in Chongqing, China. Erell et al.[5] measured two urban street canyons in central Adelaide and at two reference sites in a suburban location, and the meteorological records revealed substantial differences between air temperature in the urban street canyons and both reference sites.

Zheng et al.[6] analyzed the heat wave which occurred around Beijing city on 24 June 2009, and found that the spatial distribution of high temperature as well as the heat island effect at night in Beijing is better simulated when the original USGS land-use data substituted by a 30 m resolution local land-use data. Shem et al.[7] simulated convective precipitation for two cases (urban case and nonurban case), and found that rainfall amounts downwind of the city were higher by 10% to 13% within a strip 20–50km east of the city. Zhang et al.[8] simulated the influence of urbanization on climate at local and regional scales in Yangtze River Delta, China, the conversion of rural land to urban land cover results in significant changes to near-surface temperature, humidity, wind speed and precipitation. The mean near surface temperature in urbanized areas increases on average by $0.45 \pm 0.43^\circ\text{C}$ in winter and $1.9 \pm 0.55^\circ\text{C}$ in summer; the diurnal temperature range in urbanized areas decreases on average by $0.13 \pm 0.73^\circ\text{C}$ in winter and $0.55 \pm 0.84^\circ\text{C}$ in summer.

Zhang et al. [9] reported that urbanization and other land cover change may contribute to the observed increase of $0.12\text{K} (10 \text{ yr})^{-1}$ in the daily mean temperature, $0.20\text{K} (10 \text{ yr})^{-1}$ in the daily minimum temperature, and $0.03\text{K} (10 \text{ yr})^{-1}$ for the daily maximum surface temperature in China. Zhou et al.[10, 11] analyzed the impact of inland water body changes from 1965 to 2008 on the local climate and environment of Wuhan, which is the largest city in the geographic center of China and is adjacent to vast areas of inland water bodies.

From this study, it was found that water bodies have affected the diurnal temperature difference, while the reduction of these features had significantly affected suburban climate.

In this paper, numerical simulations of urban climate in Wuhan were performed to classify the impacts of greening area ratio.

2. Case Design

2.1 Research Area

The target area in this research was set in Wuhan, China, which is a typical city in a hot and humid climatic zone. Wuhan is located at 113°41'-115°05' East, 29°58'-31°22' North, and it lies to the east of the Jiangnan Plain at the intersection of the middle reaches of the Yangtze and Han Rivers. (Fig.1) In the past 45 years, the increase in air temperature was 3°C at a height of about 1.5 m in Wuhan city.[12]

Wuhan's climate is classified as humid subtropical with abundant rainfall and four distinctive seasons, and the area is known for its oppressively humid summers. Dew point temperatures in Wuhan often reach 26°C or more. Because of its hot summer weather, Wuhan is commonly known as one of the “Three Furnaces of China”, along with Nanjing and Chongqing. Spring and autumn are generally mild, while winter is cool with occasional snowfall. The monthly 24-hour average temperature ranges from 3.7°C in January to 28.7°C in July. The annual mean temperature is 16.6°C, the frost-free period lasts 211 to 272 days and the annual duration of sunlight is 1810 to 2100. Extreme temperatures have ranged from -18.1°C to 42.0°C. (Fig. 2)



Figure 1. Location of Wuhan.

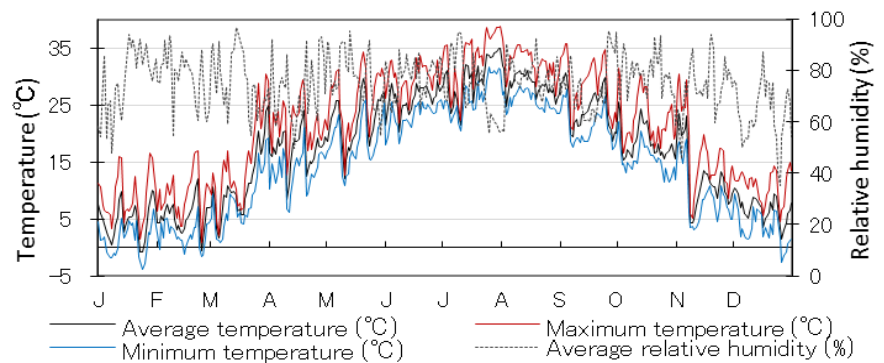


Figure 2. Daily temperature and relative humidity in Wuhan (2001).

2.2 Numerical Model

In this paper, the WRF (Weather Research and Forecasting) model system was selected as the numerical tool for our purpose. The WRF model is configured with three stage nests. The domains for the calculation were set as shown in Fig. 3.

Domain 3 included the entire area of the built-up zone of Wuhan city centered at 114.30E, 30.50N. Further details of computational domains and grid arrangements are listed in Table 1. Resolution of the horizontal grid of domain 3 was 0.5 km. The vertical dimension was non-uniform divided into 35 layers from the ground surface up to an altitude of approximately 20 km. The domain 1 run to downscale the NCEP reanalysis meteorology field and to supply initial and lateral boundary conditions for domain 2 every 6 hours, domain 2 is also supply to domain 3 like this.

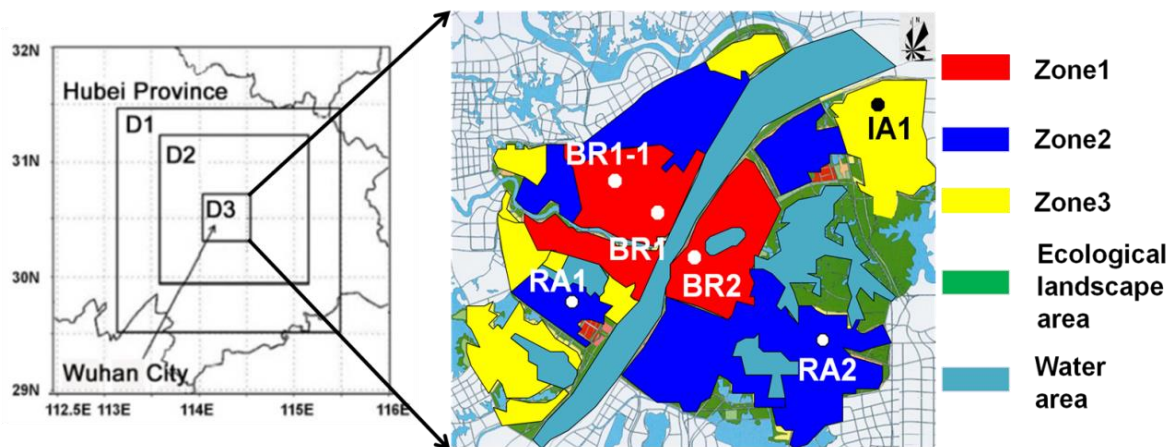


Fig. 3 Computational domains and location

The parameterization schemes used in our simulation are listed in Table 2, including long /short wave radiation processes, planetary boundary layer processes, land surface processes and microphysical processes, etc. In the WRF model, a single-layer urban canopy model [13, 14] was implemented in the NOAH land surface model to

represent the thermal and dynamic effects of urban buildings, including the trapping of radiation within the urban canopy.

Table 1 Computational domains and grid arrangements

| | Domain (X[km] x Y [km]) | Grid number (X x Y x Z) | Grid size (km) |
|----|----------------------------|----------------------------|----------------|
| D1 | 225 x 225 | 50 x 50 x 35 | 4.5 |
| D2 | 150 x 150 | 100 x 100 x 35 | 1.5 |
| D3 | 50 x 50 | 100 x 100 x 35 | 0.5 |

From weather data representative of a typical year in Wuhan, the highest temperatures are observed in July, with values above 32°C from July 23rd to July 31st. Therefore, the simulation time was set from 08:00 Local Standard Time (LST) 21st July to 08:00 LST 1th August of 2010. Model output was generated every hour. NCEP Final Operational Global Analysis data with horizontal resolution of 1°x1° in the year 2010 was used to provide initial and boundary conditions. 24 categories of land use and land cover data provided by the U.S. Geological Survey (USGS) were applied as geographic data in this study.

Table 2 WRF configurations

| | |
|----------------------|--|
| Time | 2010-07-21-08 ---- 2010-08-01-08 |
| Meteorological data | National Centers for Environmental Prediction Final Operational Global Analysis data |
| Geographic data | U.S. Geological Survey |
| Long wave radiation | RRTM longwave radiation scheme |
| Surface layer | Monin Obukhov scheme |
| Land surface | Noah land surface model+ Single layer urban canopy model (UCM) |
| Cumulus | Kain-Fritsch (new Eta) scheme |
| Short wave radiation | Dudhia scheme |
| Micro-physics | WRF Single-Moment 6-class |
| Boundary layer | Yonsei University (YSU) PBL |

2.3 Cases Design

Table 3 Case design

| | | Case 1 | Case 2 | Case 3 |
|----------------------|-------|--------|--------|--------|
| Building density [%] | Zone1 | 40 | 40 | 40 |
| | Zone2 | 35 | 35 | 35 |
| | Zone3 | 30 | 30 | 30 |
| Greening rate [%] | Zone1 | 20 | 30 | 40 |
| | Zone2 | 25 | 35 | 45 |
| | Zone3 | 30 | 40 | 50 |
| Roof_width [m] | Zone1 | 45 | 45 | 45 |
| | Zone2 | 40 | 40 | 40 |
| | Zone3 | 35 | 35 | 35 |
| Road_width [m] | Zone1 | 10 | 10 | 10 |
| | Zone2 | 10 | 10 | 10 |
| | Zone3 | 10 | 10 | 10 |
| Frc_urb [fraction] | Zone1 | 0.8 | 0.7 | 0.6 |
| | Zone2 | 0.75 | 0.65 | 0.55 |
| | Zone3 | 0.7 | 0.6 | 0.5 |

As shown in Fig. 3, Wuhan city is divided into three zones: business zone (Zone 1), residential zone (Zone 2), and industrial zone (Zone 3). According to the comprehensive planning of Wuhan city from 2010 to 2020, 3 cases were designed (Table 3). From case 1 to case 3, the building density is 40% in Zone 1, 35% in Zone 2, 30% in Zone 3; the greening area ratio is increased gradually from 20% to 40% in Zone 1, from 25% to 45% in Zone 2, and from 30% to 50% in Zone 3. In three zones, land user types are: building, green and road. Case 2 is a base case which considers the land use condition in 2020.

Table 4 Other parameters

| | Zone 1 | Zone 2 | Zone 3 |
|--|--------|--------|--------|
| Volume ratio [fraction] | 3.5 | 2.5 | 1.5 |
| Roof level [m] | 21 | 18 | 15 |
| Anthropogenic heat [W/m^2] | 140 | 60 | 40 |

| Physical Parameters | | | | | | |
|--|------|---------------|--------|-------|------|-------|
| | Roof | Building wall | Road | Water | Tree | Grass |
| Thermal conductivity [$\text{J}/(\text{m}\cdot\text{s}\cdot\text{K})$] | 0.67 | 0.67 | 0.4004 | 0.06 | 0.04 | 0.03 |
| Albedo [fraction] | 0.2 | 0.2 | 0.2 | 0.08 | 0.16 | 0.19 |
| Emissivity [fraction] | 0.9 | 0.9 | 0.95 | 0.98 | 0.3 | 0.985 |

In this paper, we compare the results at five points as shown in Fig. 2 (Zone 1: BR1, BR2; Zone 2: RA1; Zone 3: IA1, IA2). Table 4 shows all other parameters.

3. Results and Discussion

3.1 Impact of Greening Area Ratio on the Thermal Environment

Fig. 4 shows air temperature at a 2m height of domain 3 at 12:00 (LST) and 15:00 (LST) on July 31st in case 2 (2020). The maximum temperature in this case was clearly observed at 15:00. The hottest region was found in the business zones (BR1, BR2), where the air temperature exceeded 310K (37°C). Water bodies inside the urban area acted as a source of cold temperatures in the entire domain, and regions surrounding water bodies were colder than other areas.

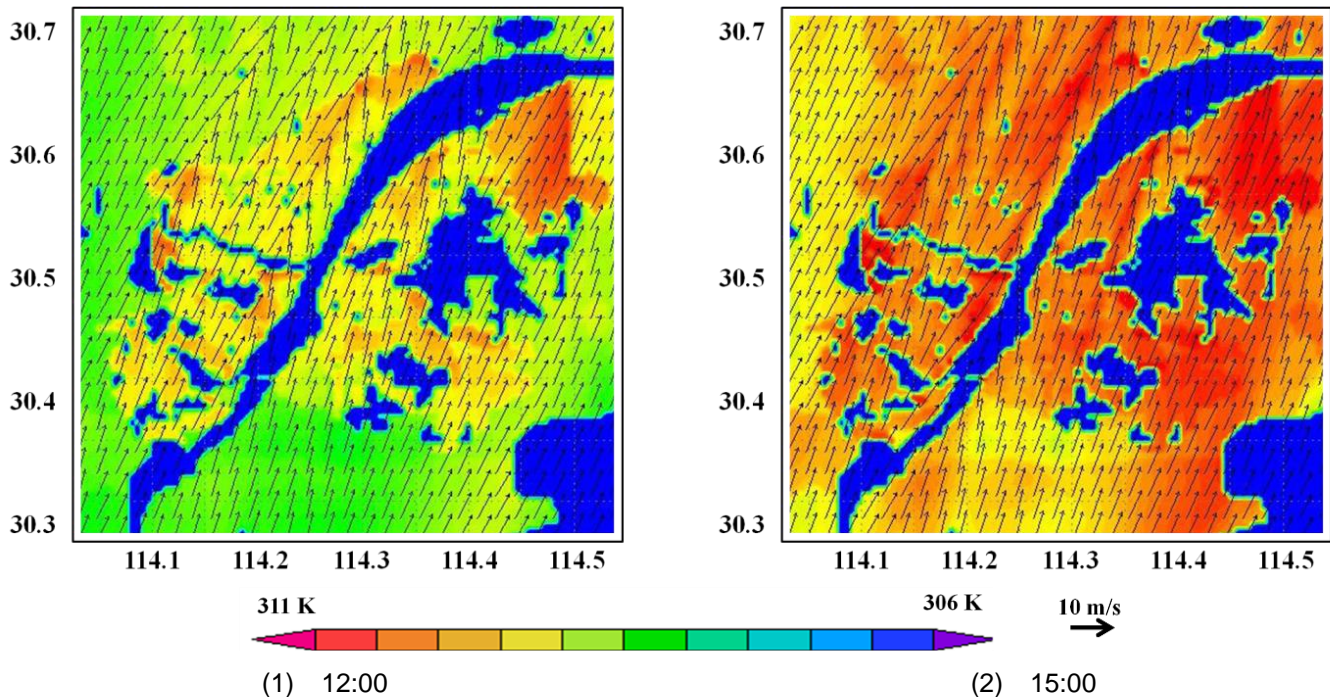


Fig. 4 Air temperature and wind velocity of domain 3 on 31st July

Fig. 5 shows the air temperature difference of each case from the value of case 2 (each case – case 2) at the height of 2 m in business zone. In business zones, green area ratio has less effect on the air temperature in the morning. In daytime, the air temperature decreases when green area ratio increases, the air temperature increases. Green area ratio has less effect on air temperature and wind velocity during the daytime, and more

effect in the nighttime. In residential zones and industrial zones, green area ratio has less effect on the air temperature in the morning. In daytime, the air temperature decreases when green area ratio increases, the air temperature increases. Green area ratio has less effect on air temperature and wind velocity during the daytime, and more effect in the nighttime

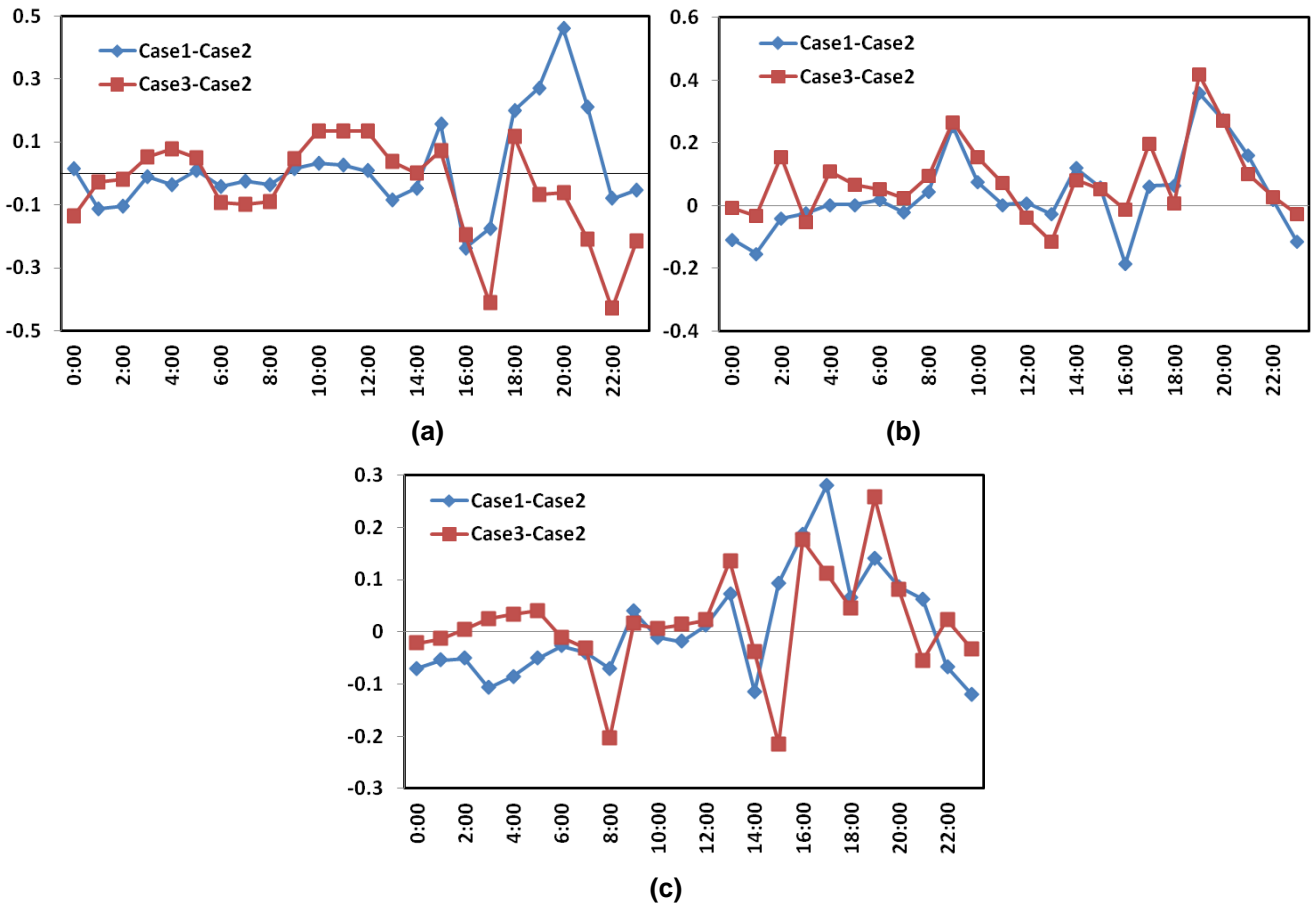
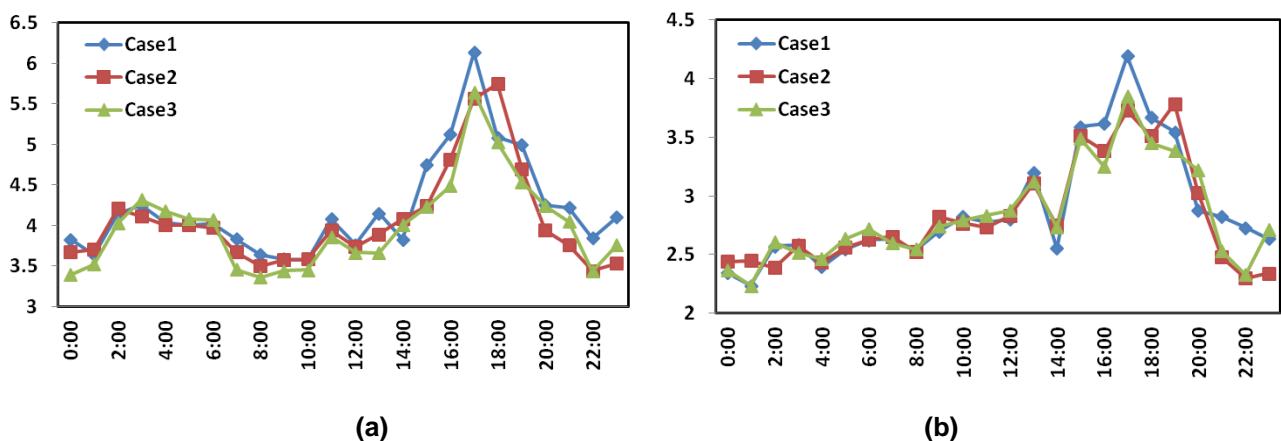


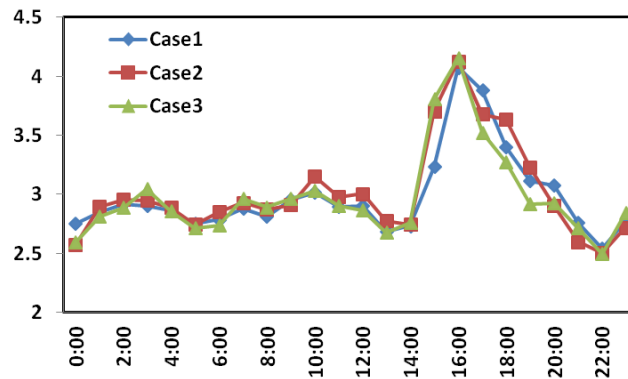
Fig. 5 Air temperature difference with case 2 (°C) of different greening rate (2m height) (a) Business zone; (b) Residential zone; (c) Industrial zone.

3.2. Impact of Greening Rate on the Wind Environment

Fig. 6 shows the wind velocity at a height of 10m. In the business zone, the impact of different green area ratio at nighttime was greater than those observed during the daytime. In the daytime, the maximum wind velocity difference was about 1.3m/s, which was observed during the hottest time of the summer at 15:00. In the nighttime, the maximum wind velocity difference was about 0.8m/s, and was observed at 22:00.

In the residential zone, the different green area ratio had a less effect on wind velocity from 0:00 to 15:00. The maximum wind velocity difference was about 0.2m/s, but after 15:00, the wind velocity difference began to increase: the maximum wind velocity difference, appearing at 18:00, was about 1.5m/s. In the industrial zone, the wind velocity changes were similar to those in the residential zone: the maximum wind velocity difference was about 1.5m/s, which also appeared at 18:00.





(c)

Fig. 6 Wind velocity (m/s) of different building densities (10m height) (a) Business zone; (b) Residential zone; (c) Industrial zone.

4. Conclusions

The impact of green area ratio on the urban climate in Wuhan city, China, was analyzed in the present study and the following conclusions can be drawn:

(1) For the thermal environment, the influence of different green area ratio on air temperature in business zones was greater than that in other zones. In the daytime, the air temperature decreased when building density increased; but at nighttime, the air temperature increased with building density. In the residential and industrial zones, different green area ratio had a lesser effect on air temperature during the daytime, and a greater effect in the nighttime.

(2) For the wind environment, the wind direction in Wuhan city was strongly affected by the Yangtze River. In business zones, the impact of green area ratio on wind velocity was greater at nighttime than that during the day. In the daytime, the maximum wind velocity difference was about 0.8m/s. In the residential and industrial zones, different green area ratio had a lesser effect on wind velocity during the daytime and a greater effect in the nighttime.

References

- 1) World Urbanization Prospects, United Nations, 2007, <http://esa.un.org/unup>.
- 2) Song X, Chen Y, Zhang N. (2011). Influences of urban development on meteorological environment: A case study of Suzhou, eastern China. *Journal of Nanjing University (Natural Sciences)*, 47(1): 51-59.
- 3) Li X, Yang X, Tang J. (2011). Multiple Urban heat islands and surface energy balance during summer in Yangtze River Delta city cluster region simulated with WRF/NCAR, *Journal of the Meteorological Sciences*, 31(4) : 441-450.
- 4) Zhang H, Sato N, Izumi T, Hanaki K, Aramaki T. (2008). Modified RAMS-urban canopy model for heat island simulation in Chongqing, China. *J Appl Meteorol*, 47:509–524.
- 5) Erell E, Williamson T. (2007). Intra-urban differences in canopy layer air temperature at a mid-latitude city. *Inter J Climatol*, 27(9):1243–1255.
- 6) Zheng Z, Gao H, Wang Z, Liu W. (2012). Numerical simulation for the urbanization effects on a heat wave event around Beijing city. *Ecology and Environmental Sciences*, 21(10): 1689 -1694.
- 7) Shem W, Shepherd M. (2008): On the impact of urbanization on summertime thunderstorms in Atlanta: two numerical model case studies. *Atmos Res*, 09.013, 2008.
- 8) Zhang N, Gao Z, Wang X, Chen Y. (2010). Modeling the impact of urbanization on the local and regional climate in Yangtze River Delta, China. *Theor Appl Climatol*, 102: 331–342.
- 9) Zhang, J., Dong W, Wu L, Wei J, Chen P, and Lee D. (2005). Impact of land use changes on surface warming in China. *Adv. Atmos. Sci.*, 22: 343-348.
- 10) Zhou XF, Ooka R, Chen H, Kawamoto Y, Kikumoto H. (2012). Impact of inland-water area changes to local climate and thermal environment of Wuhan city in China under hot weather conditions. *Seisan kenkyu*, 64(1):67-72.
- 11) Zhou XF, Ooka R, Chen H, Kawamoto Y, Kikumoto H. (2011). Impact of inland water body changes from 1965 to 2008 on local climate and environment of Wuhan, China. *Architectural Institute of Japan*, 2011.
- 12) Chen ZH. (2007). Asymmetrical Change of Urban Heat Island Intensity in Wuhan, China. *Advances in Climate Change Research*, 3: 282-286.
- 13) Kusaka H., Kimura F. (2004). Coupling a single-layer urban canopy model with a simple atmospheric model: Impact on urban heat island simulation for an idealized case. *Journal of the Meteorological Society of Japan*, 82, 67-80.
- 14) Kusaka H., Kondo H., Kikegawa Y. (2001). A simple single-layer urban canopy model for atmospheric models: Comparison with multi-layer and slab models. *Boundary-Layer Meteorology*, 101, 329-358.